Method for Characterizing the Acoustic Properties of Thin Metamaterials Capable of Attenuating Broadband Noise at Low Frequencies.

Tenon Charly Kone*[1], Sebastian Ghinet†[1], Raymond Panneton‡[2] and Anant Grewal§[1]
[1]National Research Council Canada, Flight Research Laboratory, Ottawa, Ontario, Canada.
[2]CRASH, Centre de Recherche Acoustique-Signal-Humain, Université de Sherbrooke, Sherbrooke, Québec, Canada.

1 Introduction

Attenuating noise, especially at low frequencies, poses a persistent and challenging problem across various industries such as transportation, aeronautics, and building sectors. The complexity lies in the design constraints imposed by long acoustic wavelengths associated with low frequencies, necessitating specialized approaches. This challenge becomes particularly significant when addressing noise generated by Unmanned Aerial Systems (UAS). Among the primary sources of UAS noise, the tonal noise emerges as a prominent concern. Although conventional resonators have been commonly used to tackle this issue, their effectiveness is limited by spatial constraints and their ability to attenuate only a single frequency.

In recent works by the authors [1-3], a solution that utilizes thin structuring materials was introduced, to effectively attenuate multiple resonant frequencies that could be combined to broaden the resonant attenuation frequency range of a metamaterial at low frequencies. The present study focuses on configurations comprising two parallel sub-metamaterials embedded within a layer of fiberglass. Each sub-metamaterial consists of a serial assembly of periodical unit cells, contributing to its unique acoustic properties. To evaluate the performance and potential of these metamaterial configurations, COMSOL Multiphysics finite element methods (FEM) was utilized. This approach enabled the prediction of crucial acoustic parameters, such as the normal incidence sound absorption coefficient (SAC) and sound transmission loss (STL), for each metamaterial configuration. Implementing this FEM approach for optimizing design parameters can be challenging but is crucial for accurate assessments.

The primary objective of this article is to characterize the metamaterial configurations proposed by Kone et al. [3]. Transfer matrices (TM) in series and in parallel arrangements were used to thoroughly analyze the effectiveness and applicability of these novel metamaterial designs in noise attenuation applications. Through the preliminary findings in this article, valuable insights into the potential advancements and future directions of research in the field of noise reduction are provided.

2 Materials and Methods

The metamaterial used in this study is constructed by overlaying two axisymmetric sub-metamaterials embedded in a glass wool (GW) layer of thickness t_p and the length $N\ell_{PUC}$.

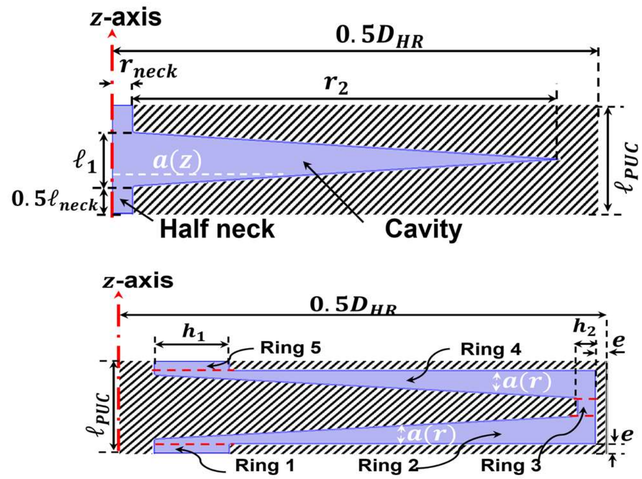

Figure 1: Top image: PUC of first sub-metamaterial. Bottom image: PUC of second sub-metamaterial. 2D-axisymmetric view.

Each sub-metamaterial consists of N periodical unit cells (PUCs).

The first sub-metamaterial's PUC (Fig. 1, top) consists of a cylindrical half neck with a radius r_{neck}, a length $0.5\ell_{nec}$. It also includes an annular cavity in the shape of an isosceles triangle of height r_2 and base $\ell_1 = \ell_{PUC} - \ell_{neck}$. In this configuration, plane wave propagation occurs along the axis of revolution, i.e. the z-axis, of the metamaterial. Therefore, the PUC was discretized perpendicular to the z-axis of revolution with transfer matrices in series. Each cell (i) has a thickness h_i and a height $a(z_i)$. The transfer matrix of cell i is given by

$$\boldsymbol{T_i} = \left[cos(k_i h_i)\; jZ_i sin(k_i h_i); \frac{jsin(k_i h_i)}{Z_i}\; cos(k_i h_i)\right],$$

where k_i and Z_i are the wave number and characteristic impedance of the effective fluid, respectively. These parameters are modeled using the Johnson Champoux Allard (JCA) model. Each cell is a cylinder of radius $a(z_i)$. Applying the Transfer Matrix Method (TMM) in series, the transfer matrix of the PUC (T_{PUC}) is obtained as the product of all T_i matrices of the elementary cell ($\boldsymbol{T_{PUC1}} = \prod_{i=1}^{N} \boldsymbol{T_i}$, where N represents the number of discretization elements). Sub-metamaterial 1 is a superposition of N_{PUC} PUCs. Finally, the TM of sub-metamaterial 1 can be expressed as $\boldsymbol{T_{meta1}} = (\boldsymbol{T_{PUC1}})^{N_{PUC}}$.

The second sub-metamaterial's PUC, as shown in Fig. 1 (bottom), was created by combining multiple rings of different geometries: (i) Ring 1: This is a simple ring geometry of rectangular cross-section. (ii) Ring 2: Following Ring 1, there is a ring with a trapezoidal cross-section. (iii) Ring 3: After Ring 2, is another ring of rectangular cross-section. (iv) Rings

*TenonCharly.Kone@nrc.gc.ca
† Sebastian.Ghinet@nrc.gc.ca
‡ Raymond.Panneton@USherbrooke.ca
§Anant.Grewal@nrc-cnrc.gc.ca

4 and 5 are the mirror images of the first two rings. According to the propagation of the wave in this sub-metamaterial two types of discretization were used. The first discretization was used for Rings 1, 3 and 5. It was perpendicular to the axis of revolution of the metamaterials as in the first sub-metamaterial. The second discretization concerned Rings 2 and 4 where the plane wave propagates radially. Thus, the type of discretization (radial discretization) used in these two rings was parallel to the axis of revolution of the metamaterials. Whatever the type of axial or radial discretization, the thickness of each cell i had a thickness h_i and a height $a(r)$. The heights $a(r)$ of the discretization of Rings 1, 3 and 5 were constant, while they vary linearly with the radius for Rings 2 and 4. As for the first sub-metamaterial, the TM of each ring j was defined as $\boldsymbol{T_{rg,j}} = \prod_{i=1}^{N} \boldsymbol{T_i}$, where N represents the number of discretization elements of the ring, and T_i the TM of the i^{th} element. Each cell is a slit of radius $a(r_i)$ with JCA effective fluid properties. By considering section-change matrix T_c (for conservation of volumetric flow) between rings, the transfer matrix of the PUC of metamaterial 2 is given by $\boldsymbol{T_{PUC2}} = \boldsymbol{T_{rg,1} T_{C1} T_{rg,2} T_{C2} T_{rg,3} T_{C3} T_{rg,4} T_{C4} T_{rg,5}}$. Finally, the TM of sub-metamaterial 2 can be expressed as $\boldsymbol{T_{meta2}} = (\boldsymbol{T_{PUC2}})^{N_{PUC}}$.

The TM of the glasswool (GW) in which both metamaterials are embedded has been analytically calculated using the JCA equivalent fluid model [4]. The resistivity of the GW was 20709 Pa*s/m^4. Knowing the TMs of each sub-metamaterial and of the GW, the global TM of the metamaterial can be calculated. Since these three elements are in parallel, the parallel transfer matrix method (PTMM) is used for their assembling [1,5].

3 Results

The sound absorption coefficients (SAC) of each sub-metamaterial, as well as the assembled metamaterial, were analyzed using the present approach (TMM-Current Model) and compared with results obtained using COMSOL FEM (Figs. 2-4). The focus was on the first two resonance frequencies. Regarding the sub-metamaterials, the TMM model accurately predicts the first two resonance frequencies, which closely match those obtained from COMSOL simulations. However, the amplitudes of these resonant frequencies are overestimated by the TMM model (Figs. 2 and 3). The present approach using the PTMM to calculate the SAC of the assembled metamaterial is also in good agreement with COMSOL mainly for the first two resonance frequencies. Moreover, as for the results obtained using COMSOL a broadening of the attenuation at the first resonant frequency can be observed (Fig. 4).

4 Conclusion

This study highlights the potential of the transfer matrix method (TMM) in analyzing complex configurations. The TMM model accurately calculated sound absorption resonant frequencies for individual sub-metamaterials, closely matching numerical FEM results with a fraction of computation time (quasi-instantaneous computation time). However, the

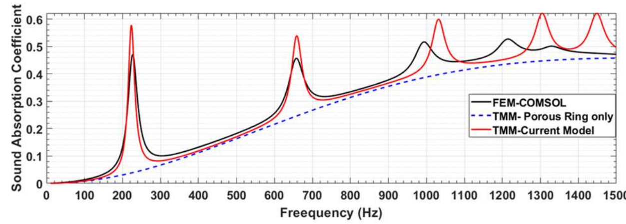

Figure 2: SAC of the first metamaterial embedded in GW layer

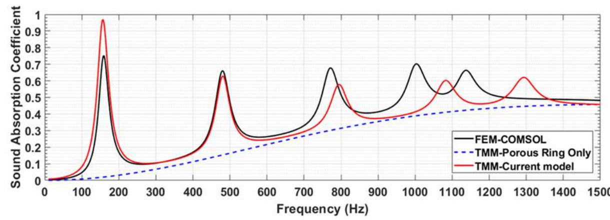

Figure 3: SAC of the second metamaterial embedded in GW layer

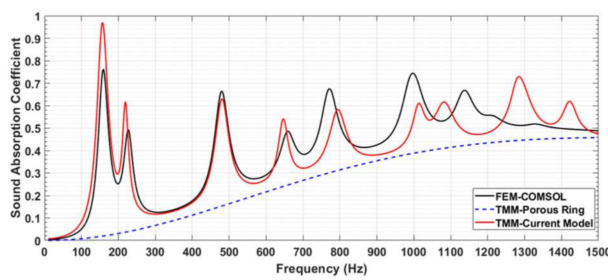

Figure 4: SAC of the metamaterial embedded on the GW layer

results obtained using the present model in terms of sound absorption coefficient of the assembled material demonstrate that some numerical improvements are still required on the proposed TM approach. Ongoing investigations aim to improve the present approach before applying it to sound transmission loss predictions. This research provides a foundation for future advancements in utilizing TMM for complex configurations and improving predictions of absorption and sound transmission properties.

References

[1] T. C. Kone, S. Ghinet, R. Panneton, T. Dupont and A. Grewal. Multi-tonal low frequency noise control using Helmholtz resonators with complex cavity designs for aircraft cabin noise improvement. NTER-NOISE 2021, vol. 263 (2), 1-5 August, Washington, US.

[2] T. C. Kone, S Ghinet, R Panneton, Z Laly, C Mechefske and A. Grewal. Control and broadening of multiple noise frequencies using an assembly of sub-metamaterials connected by membranes for aircraft noise mitigation. IinterNoise 2022, Glasgon, UK.

[3] T. C. Kone, S Ghinet, R Panneton and A. Grewal. Broadband low frequency noise attenuation using thin acoustic metamaterials for aircraft cabin noise mitigation. NTER-NOISE 2023, 20-23 August, ChiBa, Greater Tokyo, Japan.

[4] Y. Champoux and J. Allard. Dynamic tortuosity and bulk modulus in air-saturated porous media, Journal of Applied Physics, 70(4), 1975-1979 (1991).

[5] K. Verdiere, R. Panneton, S. Elkoun, T Dupont, and P. Leclaire. Transfer matrix method ap-plied to the parallel assembly of sound absorbing materials, JASA, 134, 4648-4658 (2013).